J Mater Sci (2014) 49:1317–1327
DOI 10.1007/s10853-013-7815-6

Explaining the heat capacity of wood constituents by molecular vibrations

Emil Engelund Thybring

Received: 16 July 2013 / Accepted: 9 October 2013 / Published online: 19 October 2013

Abstract The heat capacity of wood and its constituents is important for the correct evaluation of many of their thermodynamic properties, including heat exchange involved in sorption of water. In this study, the dry state heat capacity of cellulose, hemicelluloses and lignin are mathematically described by fundamental physical theories relating heat capacity with molecular vibrations. Based on knowledge about chemical structure and molecular vibrations derived from infrared and Raman spectroscopy, heat capacities are calculated and compared with experimental data from literature for a range of bio- and wood polymers in the temperature range 5–370 K. A very close correspondence between experimental and calculated results is observed, illustrating the possibility of linking macroscopic thermodynamic properties with their physical nano-scale origin.

Introduction

The heat capacity of biopolymeric substances such as wood and its constituent polymers is one of the basic thermodynamic properties, which is important for correctly calculating other thermodynamic parameters such as enthalpy and entropy in processes. For instance, knowing the heat capacity is fundamental for evaluating heat exchange involved in sorption of water. Thus, a correct mathematical description of heat capacity underpins the evaluation of a whole range of other important properties of wood. Heat capacity is a macroscopic property of materials; however, its physical origin is molecular vibrations at the nano-scale. This makes it a property that is perhaps easier to accurately measure experimentally than to accurately describe theoretically, since the latter requires fundamental knowledge of chemical structure and nano-scale behaviour of the material. The heat capacity of wood and its variation with moisture content and temperature has for more than a century been examined experimentally and several mathematical regression lines have been proposed for predicting it [1]. While such regression lines can be useful for engineering purposes, they offer no explanation or hint to the physical nano-scale origin of heat capacity, and the mechanisms causing its variation with moisture content and temperature. Several researchers have tried to examine the subject closer, e.g. Hatakeyama et al. [2] investigated heat capacity of cellulose, and Karachevtsev and Kozlov [3] attempted a mathematical description of it by some of the theories presented in this study. Nonetheless, a mathematical description of the heat capacity of wood and its constituents linking heat capacity with its physical nano-scale origin has hitherto not been presented.

In this study, the heat capacity of wood polymers will be examined from available experimental data from various literature sources. Based on knowledge about chemical structure and molecular vibrations derived from infrared and Raman spectroscopy, the heat capacity will be theoretically described using the approach of Wunderlich and co-workers [4–7]. For decades, they have examined the heat capacity of various polymers and explained their results by fundamental physical theories. This study reports

E. E. Thybring (✉)
ETH Zürich, Institute for Building Materials, Wood Materials Science, Schafmattstrasse 6, CH 8093 Zurich, Switzerland
e-mail: ethybring@ethz.ch

E. E. Thybring
EMPA-Swiss Federal Laboratories for Materials Science and Technology, Applied Wood Materials, Ueberlandstrasse 129, CH 8600 Dübendorf, Switzerland

the theoretical basis and heat capacity of dry wood constituents, whereas forthcoming publications will examine the heat capacity of wood itself and effects of moisture.

Heat capacity and molecular vibrations

The heat capacity of solid materials, i.e. the amount of energy needed to increase the temperature of a material, depends on the capacity for storing vibrational energy for instance as molecular vibrations in covalent bonds. The heat capacity of solid materials is often measured experimentally under constant pressure and denoted c_p. It is typically reported as (J/mol K) or (J/g K). The heat capacity of metals and some other materials can be described purely by molecular vibrations. For polymers, the situation is more complex since the heat capacity is based on both molecular vibrations as well as large-amplitude conformational motion, e.g. internal rotation of flexible polymers [4]. In general, the overall heat capacity at constant pressure, c_p (J/mol K) can be determined as the sum of three contributions

$$c_p = c_{vib} + c_{ext} + c_{conf}, \tag{1}$$

where c_{vib}, c_{ext} and c_{conf} are the vibrational, external and conformational contributions, respectively. All of these have the same unit as c_p.

The vibrational contribution, c_{vib} is related to molecular vibrations of the solid material. Einstein [8] described these vibrations by an assembly of one-dimensional harmonic oscillators; each atom having three motional degrees of freedom and thus each atom corresponding to three oscillators. For such assemblies the heat capacity as function of temperature is found as

$$c_{vib} = NR\frac{\left(\frac{\Theta_E}{T}\right)^2\exp\left(\frac{\Theta_E}{T}\right)}{\left(\exp\left(\frac{\Theta_E}{T}\right)-1\right)^2} = \frac{NR}{4}\left(\frac{\Theta_E}{T}\right)^2\operatorname{csch}^2\left(\frac{\Theta_E}{2T}\right), \tag{2}$$

where c_{vib} (J/mol K) is heat capacity at constant volume, N is number of oscillators, T (K) is absolute temperature and Θ_E (K) is Einstein temperature related to the average oscillator frequency by

$$\Theta_E = \frac{hcv}{k} = 1.4388\frac{\text{K}}{\text{cm}^{-1}}\cdot v, \tag{3}$$

where ν (cm^{-1}) is vibrational wavenumber, h (J s) is Planck's constant, c (m/s) is the speed of light and k (J/K) is Boltzmann's constant. This model fits experimental data for simple materials quite well above 50 K [9]. The theory of heat capacity of solid materials was further advanced by Debye [10] who described the solid by a distribution of vibrational frequencies. This theory fits the experimental data better than Eq. (2) at low temperatures. The heat capacity of the Debye model is given as

$$c_{vib} = NR\cdot D_3\left(\frac{\Theta_D}{T}\right) = 3NR\left(\frac{T}{\Theta_D}\right)^3\int_0^{\frac{\Theta_D}{T}}\frac{\left(\frac{\Theta}{T}\right)^4\exp\left(\frac{\Theta}{T}\right)}{\left(\exp\left(\frac{\Theta}{T}\right)-1\right)^2}\text{d}\left(\frac{\Theta}{T}\right), \tag{4}$$

where Θ_D (K) is Debye temperature corresponding with the maximum vibrational frequency found in the material, but otherwise calculated similar to Θ_E. The function D_3 denotes in this study the temperature derivative of the three-dimensional Debye function which also exists in a one- and two-dimensional form. The general form of the temperature derivative of Debye functions is

$$D_n\left(\frac{\Theta}{T}\right) = n\left(\frac{T}{\Theta}\right)^n\int_0^{\frac{\Theta}{T}}\frac{x^{n+1}\exp(x)}{(\exp(x)-1)^2}\text{d}x = n\left(\frac{T}{\Theta}\right)^n\int_0^{\frac{\Theta}{T}}\frac{x^{n+1}}{4}\operatorname{csch}^2\left(\frac{x}{2}\right)\text{d}x, \tag{5}$$

where n represents the dimension (1, 2 or 3). The right hand side of Eq. (5) shows a convenient mathematical rearrangement for numerical computational purposes. Often Eqs. (2) and (4) are fitted to experimental data for obtaining the average vibrational frequency or distribution of vibrational frequencies. For many polymers, however, the distribution of vibrational frequencies is already partly known from infrared and Raman spectroscopy at least in the 400–4000 cm^{-1} range (Θ = 576–5755 K). These techniques provide insight to parts of the vibrational spectrum in which vibrations of various chemical groups, e.g. vibrations related to C–H and O–H groups, are located. The lower frequency spectrum, i.e. below 400 cm^{-1} mainly contains vibrations related to skeletal deformations, e.g. deformation of aromatic rings, and can for instance be found by molecular modelling [11]. If not, the contribution of skeletal vibrations can be adequately described by the general Tarasov equation Eq. (6) [12]

$$\frac{c_{vib}(\text{skeletal})}{NR} = T\left(\frac{\Theta_1}{T},\frac{\Theta_2}{T},\frac{\Theta_3}{T}\right) = D_1\left(\frac{\Theta_1}{T}\right) - \frac{\Theta_2}{\Theta_1}\left[D_1\left(\frac{\Theta_2}{T}\right) - D_2\left(\frac{\Theta_2}{T}\right)\right] - \left(\frac{\Theta_3^2}{\Theta_1\Theta_2}\right)\left[D_2\left(\frac{\Theta_3}{T}\right) - D_3\left(\frac{\Theta_3}{T}\right)\right] \tag{6}$$

which assumes a distribution of vibrational frequencies in three parts - (1) at low frequencies: a second-order frequency distribution equivalent with the three-dimensional Debye function and a characteristic Debye temperature (frequency),

Θ_3, (2) at intermediate frequencies: a linear distribution equivalent with the two-dimensional Debye function with a Debye temperature Θ_2 and (3) at higher frequencies: a constant distribution equivalent with the one-dimensional Debye function with a Debye temperature Θ_1. The three Debye temperatures, Θ_3, Θ_2 and Θ_1 describe the maximum frequency (Debye temperature) of the corresponding distribution. For linear macromolecules it is often found that $\Theta_3 = \Theta_2$, which implies that only two frequency distributions are needed to describe the skeletal vibrations. The total number of skeletal oscillators can be separated into the different domains of the Tarasov distribution as [5]

$$N_1 = N_{sk}\left(1 - \frac{\Theta_2}{\Theta_1}\right), \quad N_2 = N_{sk}\left(\frac{\Theta_2}{\Theta_1} - \frac{\Theta_3^2}{\Theta_1\Theta_2}\right), \quad N_3 = N_{sk}\left(\frac{\Theta_3^2}{\Theta_1\Theta_2}\right). \tag{7}$$

The contribution of known vibrations, for instance group vibrations found by infrared and Raman spectroscopy, can be calculated by Eq. (2) if a single frequency can be assigned to the vibration. For some vibrations, however, a frequency range is needed to describe a particular vibration. In this case, a uniform distribution is often assumed between an upper limit (Θ_U) and a lower limit (Θ_L), and the contribution to the heat capacity can be found as

$$c_{vib}(\text{group}) = NR\frac{\Theta_U}{\Theta_U - \Theta_L}\left[D_1\left(\frac{\Theta_U}{T}\right) - \left(\frac{\Theta_L}{\Theta_U}\right)D_1\left(\frac{\Theta_L}{T}\right)\right], \tag{8}$$

where D_1 is the temperature derivative of the one-dimensional Debye function Eq. (5). For narrow frequency distributions, this reduces to the Einstein model Eq. (2).

The external contribution, c_{ext} is due to thermal expansion of the material. Since the other contributions relate to heat capacity at constant volume, c_{ext} takes into account the deviation between c_p and c_v. Analogous to the constant difference between c_p and c_v of R (= 8.3145 J/mol K) for ideal gases, the deviation between c_p and c_v for solid materials can be found as

$$c_{ext} = c_p - c_v = \frac{TV\alpha^2}{\beta_T}, \tag{9}$$

where V (m^3/mol) is molar volume, α (K^{-1}) is thermal expansivity and β_T (Pa^{-1}) is isothermal compressibility. If these parameters are not available, it is possible to describe c_{ext} by the Nernst–Lindemann approximation [13] modified by Pan et al. [14]

$$c_{ext} = c_p - c_v = 3RA_0\frac{c_p^2}{c_v}\frac{T}{T_m}, \tag{10}$$

where $A_0 = 0.0039$ mol K/J [14], and T_m (K) is equilibrium melting (glass transition) temperature of the chemical substance. A_0 is given per mole of vibrating atoms. Based on experimental data for c_p at given temperatures, Eq. (10) can be rearranged and c_v and subsequently c_{ext} can be calculated.

The conformational contribution, c_{conf} is related to large-amplitude conformational motion of polymeric segments, e.g. rotation of chemical groups or the polymeric backbone [4], and it can be found by statistical mechanics [15, 16]. The basic simplifying assumption is that the conformational states of bonds, flexible segments or repeating unit can exist in two different states: the ground state and an excited state of higher energy than the ground state. From this assumption, the conformational contribution can be calculated. For non-cooperative rotations in polymers, i.e. where rotation of one bond or segment does not influence that of its neighbours, the conformational contribution [16, 17] is given by

$$c_{conf} = nR\frac{\Gamma\left(\frac{\Theta_C}{T}\right)^2\exp\left(\frac{\Theta_C}{T}\right)}{\left(\exp\left(\frac{\Theta_C}{T}\right) + \Gamma\right)^2}, \tag{11}$$

where Γ is degeneracy ratio, i.e. ratio of number of available excited states to that of available ground states, n is number of mobile chain units per repeating unit and Θ_C (K) is temperature associated with change in conformation given as

$$\Theta_C = \frac{e_2 - e_1}{N_A k}, \tag{12}$$

where e_2 and e_1 (J/mol) are energies of excited and ground states, respectively, and N_A (mol^{-1}) is Avogadro's constant. For cooperative rotations, i.e. where neighbouring segments influence rotations of the segment in question, the heat capacity contribution can be described by [15]

$$c_{conf} = N_A\frac{d}{dT}\left(-kT^2\frac{d(F_{conf}/kT)}{dT}\right), \tag{13}$$

where

$$F_{conf} = -kT\ln\left(\frac{1}{2}\left[1 + \exp\left(\frac{-\Theta_A - \Theta_B}{T}\right)\Gamma + \sqrt{\left(1 + \exp\left(\frac{-\Theta_A - \Theta_B}{T}\right)\Gamma\right)^2 - 4\Gamma\left(\exp\left(\frac{-\Theta_A - \Theta_B}{T}\right) - \exp\left(\frac{-\Theta_B}{T}\right)\right)}\right]\right), \tag{14}$$

Table 1 Overview of experimental data used in this study

Material	Data used for assessing	Temperature range (K)	T_m (K)	References
Microcrystalline cotton cellulose	Cellulose	5–370	515	[30]
		80–370		[31]
Wood sulphite cellulose	Cellulose	5–370	515	[30]
Straw cellulose	Cellulose	80–370	515	[30]
Amorphous wood cellulose	Cellulose, hemicelluloses	80–370	515[a]	[30]
Crystalline α-D-glucose	Hemicelluloses	7–350	312	[32]
Crystalline sucrose	Hemicelluloses	5–340	343	[33]
Crystalline α-D-xylose	Hemicelluloses	2–300	285	[34]
Cupro-ammonium lignin	Lignin	8–370	461	[35]
Sulphuric lignin	Lignin	80–370	461	[35]

The equilibrium melting (glass transition) temperature, T_m is taken from [20, 36–40]

[a] Despite its amorphous nature, molecular modelling and experimental results [41] indicate that the glass transition temperature is similar to that of crystalline cellulose

where $\Theta_A = \frac{A}{N_A k}$ and $\Theta_B = \frac{B}{N_A k}$, where B (J/mol) is difference in energy level between excited and ground states, and A (J/mol) takes into account the cooperativity of neighbouring segments.

Experimental data and calculation method

The experimental data used in this study to correlate heat capacity and molecular vibrations are taken from various literature sources and shown in Table 1. No experimental data could be found for wood hemicelluloses. Therefore, a range of variously sized sugar oligomers are included, Table 1. The computer software MATLAB R2012b was used for all numerical calculations.

For all substances, a proper molecular unit representing each polymer is selected. For cellulose, half a cellobiose unit is used, whereas lignin is attempted modelled using a simple coniferyl alcohol. For hemicelluloses, the molecular units of galactoglucomannan and arabinoxylan as given by Sjöström [18] are used. For the small sugar oligomers, the entire molecules are selected as molecular units. Based on molar mass of each molecular unit, the experimental data are converted to (J/mol K). The first step in evaluating the different heat capacity contributions is conversion of experimental c_p to c_v by Eq. (10) using T_m given in Table 1.

The vibrational contribution from group vibrations, c_{vib} (group) is determined from vibrational spectra for each molecular unit. These are illustrated in Fig. 1 for the four main wood polymers: cellulose, glucomannan, xylan and lignin. The various vibrations have been selected in accordance with literature sources quoted in Table 2. In Fig. 1 and Table 2, vibrational frequencies along with the number of oscillators for each molecular unit are given. For cellulose, the selected molecular unit ($C_6H_{10}O_5$) contains 21 atoms, and therefore its total number of oscillators is 63. Of these, Table 2 identifies 42 group vibrations, whereas the remaining 21 vibrations are skeletal vibrations. Group vibrations designated in Table 2 by a frequency range are modelled by Eq. (8), while those with a single assigned frequency are modelled by Eq. (2). By subtracting c_{vib} (group) from the converted experimental c_v, the vibrational contribution from skeletal vibrations, c_{vib} (skeletal) is evaluated. At temperatures below 200 K, the skeletal contribution dominates and this is found by fitting Eq. (6) to the $c_v - c_{vib}$ (group) data in the 5–200 K range in accordance with Pyda [4]. If the remaining difference $c_v - c_{vib}$ (group) $- c_{vib}$ (skeletal) is significant at temperatures above 200 K, conformational contributions are calculated. As a last step, the total calculated c_v including group, skeletal vibrations and potentially conformational contributions is converted to c_p by use of Eq. (10) for direct comparison with experimental c_p data.

Results and discussion

In the following, the experimental data points are so close that they are illustrated by continuous lines rather than by individual markers.

In Fig. 2, experimental and calculated heat capacities of microcrystalline cotton cellulose are shown along with contributions from group and skeletal vibrations; the latter based on Debye temperatures from Table 3. A very close correspondence between experimental and calculated results is seen similar to that found for organic polymers [19]. It is clear that skeletal vibrations mainly contribute in the 5–200 K range, whereas the change in heat capacity with temperature above 250 K is due to group vibrations. This change in behaviour from one dominated by skeletal to group vibrations is typical [5, 19], since the previous

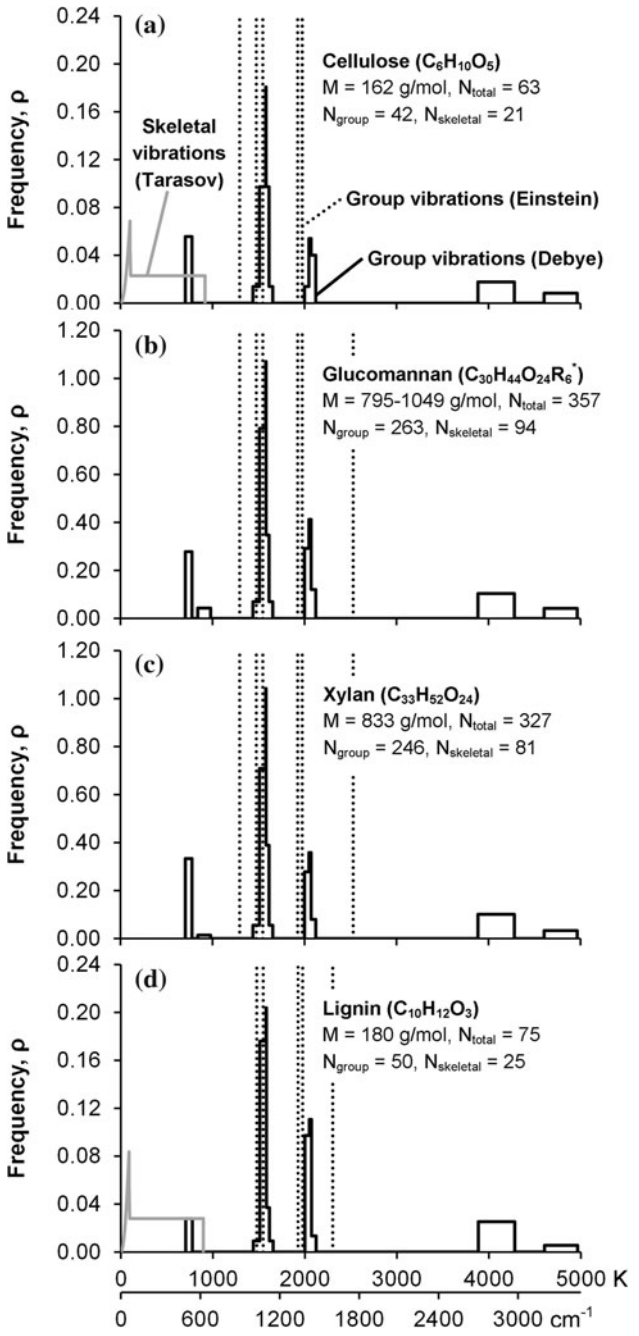

Fig. 1 Vibrational spectrum of selected molecular units for **a** cellulose, **b** galactoglucomannan, **c** arabinoxylan and **d** lignin illustrating both skeletal and group vibrations. *For galactoglucomannan an average value for the number of vibrators for each vibration is used based on an equal distribution of R = CH_3CO and R = H

have vibrational frequencies in the lower frequency range. Therefore, these vibrations are excited before the group vibrations. No conformational contribution is needed to accurately describe the heat capacity in Fig. 2, presumably due to restrictions on conformational motions of aggregated crystalline polymers.

The very close correspondence between experiment and theory is also seen for heat capacities of other types of cellulose and lignin shown in Fig. 3. Skeletal vibrations of cellulose in Fig. 3b, d have been calculated using average Debye temperatures for microcrystalline cotton cellulose and wood sulphite cellulose, given in Table 3, while skeletal vibrations of lignin in Fig. 3f have been modelled by Debye temperatures for cupro-ammonium lignin, also in Table 3. This is because the experimental data for these substances include the temperature range 5–80 K, and therefore presumably yield more reliable estimates of skeletal vibrations. This does not, however, affect the calculated results significantly. Debye temperatures in Table 3 for skeletal vibrations of the crystalline polymers share many similarities. For instance, they are all dominated in terms of fraction of vibrations by Θ_1 and have $\Theta_2 = \Theta_3$ which is typical for linear macromolecules [5]. This is somewhat surprising for lignin, which is not a linear polymer. Furthermore, the Debye temperatures are reasonably similar between the different polymers with $\Theta_1 = 873.5 \pm 41.8$ K, $\Theta_2 = \Theta_3 = 97.8 \pm 17.4$ K for all crystalline polymers.

The only significant deviations between experimental and calculated results are seen for amorphous cellulose in Fig. 3c above 235 K, where the experimental c_p is increasingly larger than calculated results as temperature increases. This is in line with observations made by Hatakeyama et al. [2] and Uryash et al. [20]. Furthermore, experimental data for amorphous cellulose in the 80–200 K temperature range is best fitted with skeletal vibrations described by only a uniform frequency distribution, i.e. $\Theta_2 = \Theta_3 = 0$, and $\Theta_1 = 895.2$ K. Similarly, Pyda [21] found that the skeletal vibrations of amorphous, dry starch deviated from $\Theta_2 = \Theta_3$, however, three non-zero Debye temperatures were needed to describe the skeletal contribution. These deviations from the behaviour of crystalline polymers can perhaps be ascribed to the amorphous nature of the starch and cellulose investigated. However, since experimental data for the latter lacks below 80 K, the fit is uncertain. Nonetheless, if Debye temperatures for microcrystalline cellulose are used, little difference is seen in the fit to experimental data, Fig. 4. In both cases, some of the experimental data remains unexplained which is also the case for amorphous, dry starch above 250 K [21]. The unexplained part, c_v (other) is illustrated in Fig. 5 and is attributed to conformational motion due to a greater mobility of bonds and/or polymer segments [4, 15] of amorphous cellulose compared with crystalline cellulose.

Conformational motion is often linked with glass transition, where polymer mobility increases significantly seen as viscous mechanical behaviour and an increase in heat capacity. However, even below the glass transition point, secondary transitions can be seen with mechanical and

Table 2 Group vibrations in the 400–4000 cm^{-1} range assigned by experimental infrared and Raman spectroscopic studies [21, 42–49]

Vibration mode	Wavenumber (cm^{-1})	Frequency, Θ (K)	Group vibrations, N_{gr}			
			Cellulose	Glucomannan	Xylan	Lignin
O–H stretch	3200–3450	4604–4964	3	15	12	2
C–H stretch	2700–2975	3885–4280	7	41	40	10
C=O stretch	1758	2529	0	3	1	0
C=C stretch	1600	2302	0	0	0	4
C–C stretch	1050–1100	1511–1583	5	31	27	5
C–OH stretch	1000–1150	1439–1655	3	15	12	2
C–OC stretch	900, 1097–1122	1295, 1578–1614	1, 3	10, 10	12, 12	1
C–H bend	1050–1100, 1075, 1373, 1390–1440	1511–1583, 1547, 1975, 2000–2072	1, 4, 4, 1	21, 20, 20, 21	20, 20, 20, 20	7, 3, 3, 7
O–H bend	1026, 1338, 1373, 1423–1475	1476, 1925, 1975, 2047–2122	1, 1, 1, 3	7, 7, 7, 9	6, 6, 6, 6	1, 1, 1, 1
C=O bend	584–681	840–980	0	6	2	0
C–O–C bend	490–540	705–777	4	20	24	2
		N_{gr}	42	263	246	50
		$N_{skeletal}$	21	94	81	25

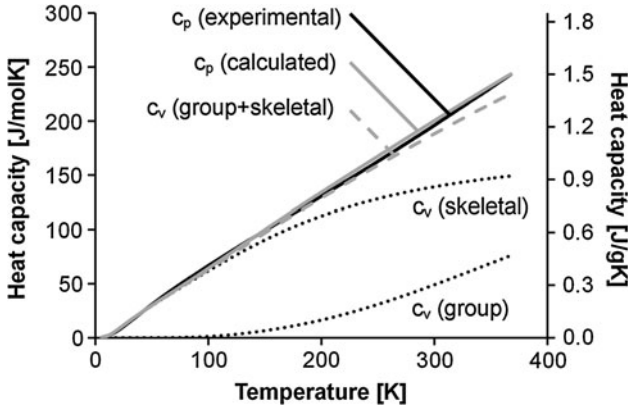

Fig. 2 Calculated c_p and c_v for cellulose based on contributions from group and skeletal vibrations. Experimental data included for microcrystalline cotton cellulose from [30]

Table 3 Debye temperatures and associated number of skeletal vibrations

Material	Θ_1 (K)	Θ_2 (K)	Θ_3 (K)	N_{sk}	N_1	N_2	N_3
Microcrystalline cotton cellulose	918.1	103.2	103.2	21	18.6	0.0	2.4
Wood sulphite cellulose	914.2	101.9	101.9	21	18.7	0.0	2.3
Amorphous wood cellulose[a]	895.2	0.0	0.0	21	21.0	0.0	0.0
Crystalline α-D-glucose	846.6	103.1	103.1	23	20.2	0.0	2.8
Crystalline sucrose	850.1	121.1	121.1	44	37.7	0.0	6.3
Crystalline α-D-xylose	816.0	69.5	69.5	18	16.5	0.0	1.5
Cupro-ammonium lignin	896.1	88.1	88.1	25	22.5	0.0	2.5

Based on data from [30, 32–35] for the range 1–200 K

[a] The skeletal contribution for amorphous wood cellulose was evaluated both by fitting Eq. (6) to experimental data in the 80–200 K range and using Debye temperatures for microcrystalline cotton cellulose

dielectric spectroscopic techniques [22]. Whereas glass transition itself is referred to as the α-relaxation, secondary relaxations are termed β-, γ- and δ-relaxations dependent on their temperature proximity to the α-relaxation. Secondary relaxations have been found in both cellulose and lignin in their native form [23]. For the latter, β-relaxation is found in the 153–223 K temperature range centred around 187 K [23], and can be attributed to OH-group mobility [24]. Thus, this motion may already be at least partly included as OH-vibrations in the heat capacity calculations, and might explain why no conformational contribution is needed to explain the experimental data of lignin. Crystalline and amorphous cellulose exhibit two secondary transitions in the 103–273 K range [23]: γ-relaxation around 150 K and β-relaxation around 213–253 K [25–27]. These are related to rotational motion of CH_2OH-groups relative to the sugar rings and rotation of the glycosidic C–O–C bond between neighbouring sugar rings, respectively [22, 25, 26]. The intensity of these transitions when measured with dielectric spectroscopy is, however, considerably larger for amorphous than for crystalline cellulose. For instance, one study shows that amorphous cellulose would have a β-relaxation intensity of 4–5 times greater than that for wood cellulose with 67 % crystallinity [28]. Thus, while crystalline cellulose might

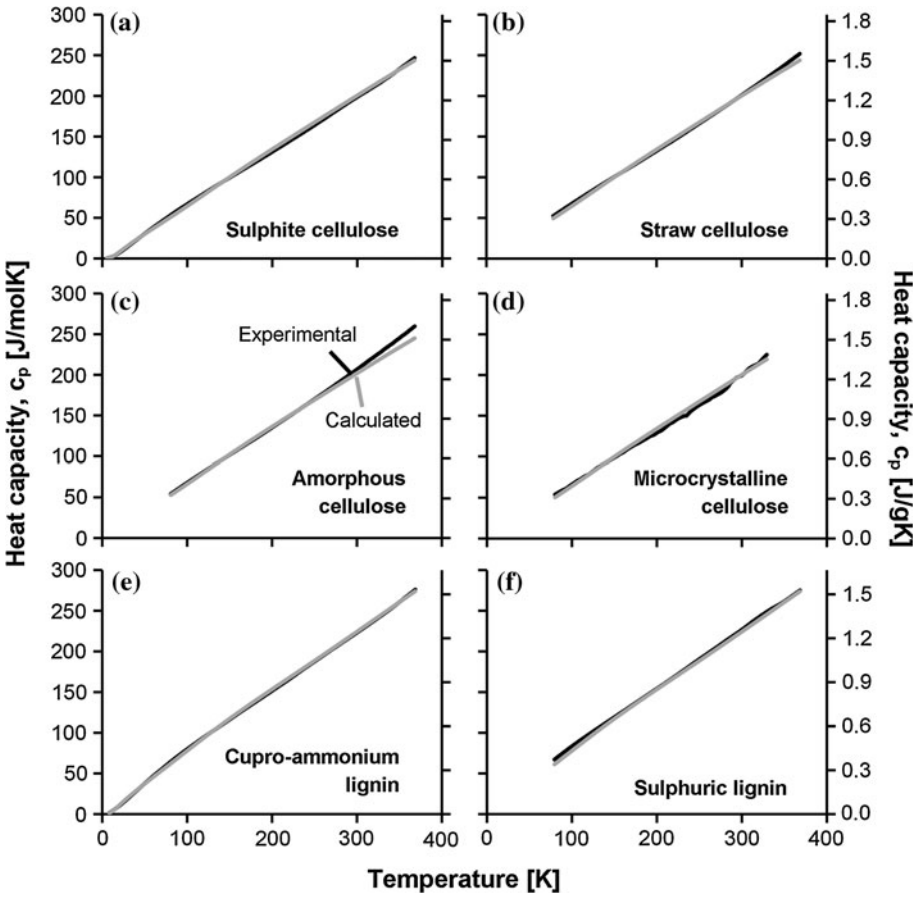

Fig. 3 Calculated and experimental c_p for **a**–**d** cellulose of various origin, and **e**, **f** lignin extracted by two different methods. Based on data from **a**–**c** [30], **d** [31], **e**, **f** [35]

experience an increase in conformational motion, this effect is considerably greater for amorphous cellulose. This can then explain why conformational contributions are only significant for amorphous and not for crystalline substances.

The two secondary transitions of amorphous cellulose have been characterised by energy differences between ground and excited states of 7–9 and 4–8 kJ/mol for the γ- and β-relaxations, respectively [25–27]. The previous shows no cooperativity and has a degeneracy ratio, Γ of 2/1, i.e. two excited states and one ground state. The latter shows cooperativity with $\Gamma = 4/1$ [25]. The influence of cooperative and non-cooperative motions on the heat capacity was fitted using $\Gamma = 2$ and 4, respectively, and varying the energy differences Θ_C, Θ_A and Θ_B without constraints. Figure 5 illustrates the best fit to c_v (other) when using Debye temperatures for either microcrystalline cellulose (Fig. 4a) or amorphous cellulose (Fig. 4b) to describe the skeletal vibrations. In the latter case, no good fit to c_v (other) could be achieved, indicating that amorphous cellulose is in fact characterised by the same skeletal vibrations as crystalline cellulose. The best fit was achieved with a contribution from combined non-cooperative and cooperative motion with $\Theta_C = 1358.6$ K (11.3 kJ/mol), $\Theta_A = -1308.1$ K (−10.9 kJ/mol) and $\Theta_B = 2120.2$ K (17.6 kJ/mol) or with only cooperative motions described by $\Theta_A = -921.6$ K (−7.7 kJ/mol) and $\Theta_B = 1745.3$ K (14.5 kJ/mol). In both cases, the overall energy barrier $\Theta_A + \Theta_B$ was around 818 K (6.8 kJ/mol) in line with values for the β-relaxation [25]. The value of Θ_C is outside the range given in Montes and Cavaille [26], however, as indicated in Fig. 5, the cooperative motion described by only Θ_A and Θ_B fits the unexplained c_v (other) equally well as the combined cooperative and non-cooperative motions described by Θ_A, Θ_B and Θ_C. Non-cooperative motion alone was unable to explain c_v (other) as seen clearly in Fig. 5. Thus, the conformational contribution to amorphous cellulose heat capacity is dominated by the cooperative motion of the β-relaxation, perhaps with a small influence of non-cooperative motion from the γ-relaxation. Figure 6 shows the different heat capacity contributions and overall fit between experimental and calculated results for amorphous cellulose. A nearly perfect fit to experimental data is seen in the entire temperature range.

A significant part of wood is made up by hemicelluloses, for softwood primarily arabinoxylan and galactoglucomannan. Despite lack of experimental data for these compounds, it is possible to predict their heat capacity based on estimates of the various contributions from skeletal and group vibrations as well as conformational

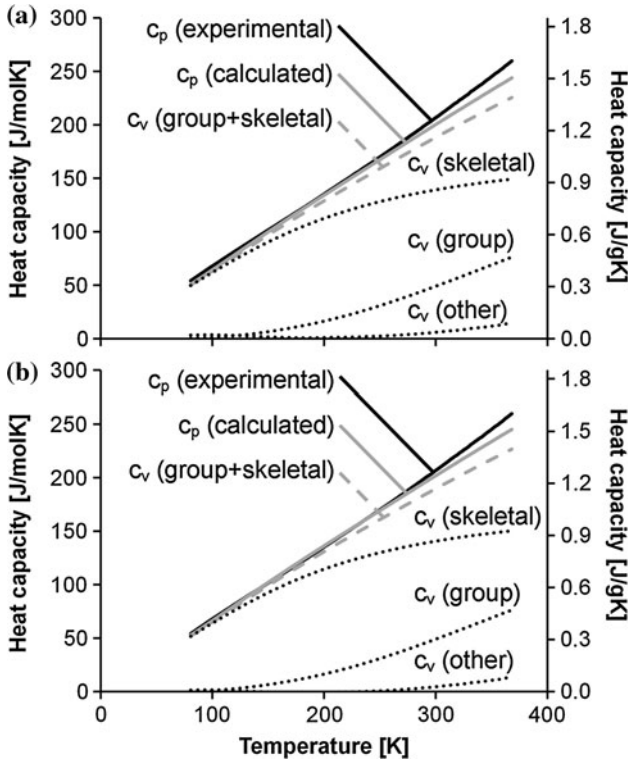

Fig. 4 Calculated c_p and c_v for amorphous cellulose based on contributions from group vibrations as well as from skeletal vibrations described by Eq. (6) for **a** microcrystalline cotton cellulose, and **b** the amorphous cellulose itself. Experimental data included for amorphous wood cellulose from [30]. c_v (other) constitutes the unexplained difference between experimental and calculated results

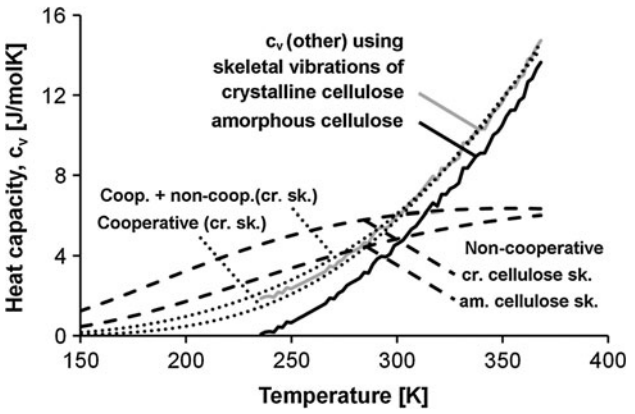

Fig. 5 Fit to c_v (other) with conformational contributions from both cooperative and non-cooperative motions

motion. The external contribution is as for the other compounds found by Eq. (10). In the temperature range 1–400 K, the different contributions have been calculated and results are shown in Fig. 8. In order to compare the different wood constituents, contributions are only shown

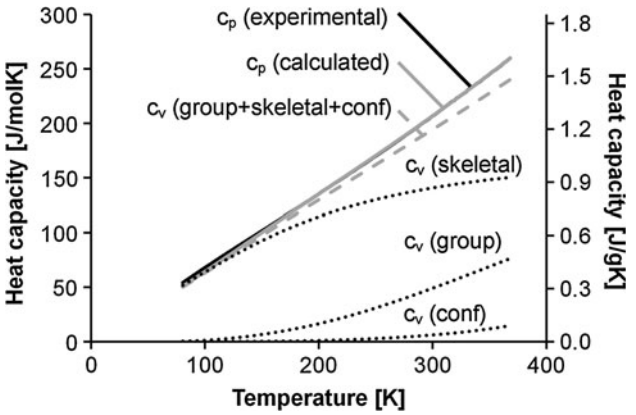

Fig. 6 Calculated c_p and c_v for cellulose based on contributions from group and skeletal vibrations and conformational motion. Experimental data included for amorphous wood cellulose from [30]

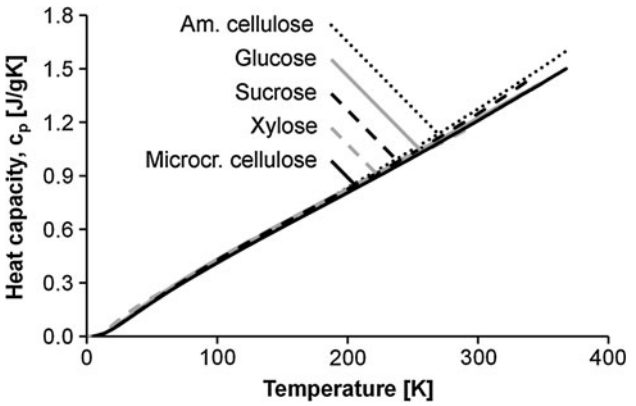

Fig. 7 Experimental data for c_p (J/g K) for variously sized sugar polymers compared with those of microcrystalline and amorphous cellulose

as (J/g K). The skeletal vibrational contribution of the hemicelluloses is found by fitting experimental data for microcrystalline cotton cellulose in the 5–200 K range with Eq. (6) after subtraction of the cellulose group vibrational contribution. This is due to the close similarity of heat capacities for the various sugar polymers seen in this temperature range in Fig. 7. This results in almost similar $\Theta_2 = 166.5$–167.2 K and $\Theta_3 = 61.9$–62.6 K while Θ_1 was found to 666.5 K and 634.1 K for glucomannan and xylan, respectively. While this fitting is not based on actual experimental data for any of the two hemicelluloses, the Debye temperatures are not far from those reported for dry, amorphous starch [21] of $\Theta_1 = 795.5$ K, $\Theta_2 = 159$ K and $\Theta_3 = 58$ K.

The group vibrational contribution to the heat capacities of glucomannan and xylan was calculated based on vibrational spectra given in Fig. 1 and Table 2. Secondary transitions attributed to rotation of CH_2OH-groups in

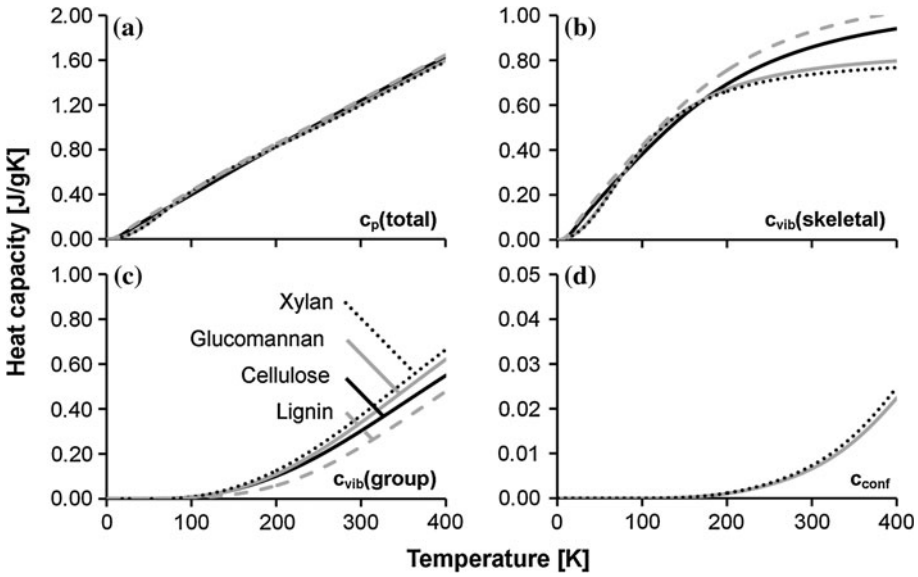

Fig. 8 Predicted heat capacities (J/g K) for the four major wood constituents: **a** total c_p, **b** skeletal vibrational contribution, **c** group vibrational contribution, **d** conformational contribution

hemicelluloses have been reported for dry wood around 175 K [29]. The conformational contribution to the heat capacity is therefore calculated by Eq. (11) using $\Theta_C = 1149.4$ K as for amorphous cellulose. For the glucomannan molecular unit, four such groups are found, i.e. $n = 4$ in Eq. (11), while only one is present in the xylan molecular unit. No secondary transition related to β-relaxation is observed in the temperature range 120–280 K when wood is completely dry [29]. Introduction of slight amounts of moisture (0.5–0.7 % moisture content) does, however, result in β-relaxation around 220–240 K. This indicates that rotation of sugar rings relative to neighbouring rings is restricted for in situ hemicelluloses in completely dry wood. Nonetheless, an additional conformational contribution is assumed in this study for both glucomannan and xylan described by similar values of Θ_A and Θ_B as for amorphous cellulose. While the actual values for glucomannan and xylan undoubtedly differ from these, the conformational contribution from β-relaxation is likely of similar magnitude.

The total heat capacity for all four major wood constituents is shown in Fig. 8a, and although the curves look quite similar, the composition between different contributions vary slightly between constituents as seen in Fig. 8b–d. This overall similarity in heat capacity can of course be attributed to similarity in chemical structure, with the slight variations being due to small differences in vibrational spectra seen in Fig. 1. From Fig. 8b–d it is clear that the skeletal and group vibrations dominate, while the conformational contribution is close to negligible. This is of course only true for polymers in the solid state, whereas the contribution is highly significant in the liquid state, i.e. above the melting temperature of the polymer.

In general, the close correspondence between experimental and calculated results shown in this study for a range of biopolymers in their dry state, illustrates the possibility of describing heat capacities of complex macromolecules by fundamental physical theories, thus linking macroscopic thermodynamic properties with their physical nano-scale origin. Moreover, it provides a baseline for evaluating effects of water on the heat capacity of wood.

Conclusion

Heat capacities in the dry state of the four major wood constituents: cellulose, glucomannan, xylan and lignin have been mathematically described using fundamental physical theories relating heat capacity with molecular vibrations. Based on knowledge about chemical structure and molecular vibrations derived from infrared and Raman spectroscopy, heat capacities have been calculated and compared with experimental data from literature for a range of bio- and wood polymers in the temperature range 5–370 K. A very close correspondence between experimental and calculated results has been observed, hereby illustrating the possibility of linking macroscopic thermodynamic properties with their physical nano-scale origin. No experimental data for glucomannan and xylan were available, but based on findings for cellulose and other variously sized sugar polymers, the heat capacities of these substances were predicted.

Acknowledgements This paper is a result of work done while the author was employed at the Department of Civil Engineering, Technical University of Denmark.

References

1. Steinhagen HP (1977) Thermal conductive properties of wood, green or dry, from −40 °C to 100 °C—a literature review. General technical report FPL-9, USDA Forest Service, Madison, WI
2. Hatakeyama T, Nakamura K, Hatakeyama H (1982) Studies on heat-capacity of cellulose and lignin by differential scanning calorimetry. Polymer 23:1801–1804
3. Karachevtsev VG, Kozlov NA (1974) Study of thermodynamic properties of cellulose at low-temperatures. Vysokomol Soedin Ser A 16:1892–1897
4. Pyda M (2002) Conformational heat capacity of interacting systems of polymer and water. Macromolecules 35:4009–4016. doi:10.1021/ma0118466
5. Pyda M, Bartkowiak M, Wunderlich B (1998) Computation of heat capacities of solids using a general Tarasov equation. J Therm Anal Calorim 52:631–656. doi:10.1023/a:1010188110516
6. Wunderlich B (1997) The heat capacity of polymers. Thermochim Acta 300:43–65. doi:10.1016/s0040-6031(96)03126-7
7. Wunderlich B (1995) The ATHAS database on heat-capacities of polymers. Pure Appl Chem 67:1019–1026. doi:10.1351/pac199567061019
8. Einstein A (1906) The Planck theory of radiation and the theory of specific heat. Ann Phys Berlin 22:180–190
9. Blackman M (1941) The theory of the specific heat of solids. Rep Prog Phys 8:11–30
10. Debye P (1912) The theory of specific warmth. Ann Phys Berlin 39:789–839
11. Sallamie N, Shaw JM (2005) Heat capacity prediction for polynuclear aromatic solids using vibration spectra. Fluid Phase Equilib 237:100–110. doi:10.1016/j.fluid.2005.07.022
12. Tarasov VV (1952) Metasilicate chains and the theory of thermal capacity. Dokl Akad Nauk SSSR 84:321–324
13. Nernst W, Lindemann FA (1911) Specific heat and quantum theory. Z Elektrochem Angew P 17:817–827
14. Pan R, Nair MV, Wunderlich B (1989) On the c_p to c_v conversion of solid linear macromolecules II. J Therm Anal 35:955–966. doi:10.1007/bf02057252
15. Pyda M, Wunderlich B (1999) Computation of heat capacities of liquid polymers. Macromolecules 32:2044–2050. doi:10.1021/ma9816620
16. Loufakis K, Wunderlich B (1988) Computation of heat-capacity of liquid macromolecules based on a statistical mechanical approximation. J Phys Chem 92:4205–4209. doi:10.1021/j100325a042
17. O'Reilly JM (1977) Conformational specific heat of polymers. J Appl Phys 48:4043–4048. doi:10.1063/1.323444
18. Sjöström E (1993) Wood chemistry—fundamentals and applications, 2nd edn. Academic Press, San Diego, p 293
19. Di Lorenzo ML, Zhang G, Pyda M, Lebedev BV, Wunderlich B (1999) Heat capacity of solid-state biopolymers by thermal analysis. J Polym Sci Pol Phys 37:2093–2102. doi:10.1002/(sici)1099-0488(19990815)37:16<2093:aid-polb12>3.0.co;2-2
20. Uryash VF, Rabinovich IB, Mochalov AN, Khlyustova TB (1985) Thermal and calorimetric analysis of cellulose, its derives and their mixtures with plasticizers. Thermochim Acta 93:409–412. doi:10.1016/0040-6031(85)85103-0
21. Pyda M (2001) Conformational contribution to the heat capacity of the starch and water system. J Polym Sci Pol Phys 39:3038–3054. doi:10.1002/polb.10060
22. Kaminski K, Kaminska E, Ngai KL, Paluch M, Wlodarczyk P, Kasprzycka A, Szeja W (2009) Identifying the origins of two secondary relaxations in polysaccharides. J Phys Chem B 113:10088–10096
23. Jafarpour G, Dantras E, Boudet A, Lacabanne C (2008) Molecular mobility of poplar cell wall polymers studied by dielectric techniques. J Noncryst Solids 354:3207–3214
24. Roig F, Dantras E, Grima-Pettenatti J, Lacabanne C (2012) Analysis of gene mutation in plant cell wall by dielectric relaxation. J Phys D Appl Phys 45. doi:10.1088/0022-3727/45/29/295402
25. Montes H, Mazeau K, Cavaille JY (1997) Secondary mechanical relaxations in amorphous cellulose. Macromolecules 30:6977–6984
26. Montes H, Cavaille JY (1999) Secondary dielectric relaxations in dried amorphous cellulose and dextran. Polymer 40:2649–2657
27. Montes H, Mazeau K, Cavaille JY (1998) The mechanical beta relaxation in amorphous cellulose. J Noncryst Solids 235:416–421. doi:10.1016/s0022-3093(98)00600-0
28. Einfeldt J, Meissner D, Kwasniewski A (2004) Molecular interpretation of the main relaxations found in dielectric spectra of cellulose—experimental arguments. Cellulose 11:137–150. doi:10.1023/B:CELL.0000025404.61412.d6
29. Obataya E, Norimoto M, Tomita B (2001) Mechanical relaxation processes of wood in the low-temperature range. J Appl Polym Sci 81:3338–3347
30. Blokhin AV, Voitkevich OV, Kabo GJ, Paulechka YU, Shishonok MV, Kabo AG, Simirsky VV (2011) Thermodynamic properties of plant biomass components. Heat capacity, combustion energy, and gasification equilibria of cellulose. J Chem Eng Data 56:3523–3531. doi:10.1021/je200270t
31. Ur'yash VF, Larina VN, Kokurina NY, Novoselova NV (2010) The thermochemical characteristics of cellulose and its mixtures with water. Russ J Phys Chem A 84:915–921. doi:10.1134/s0036024410060051
32. Boerio-Goates J (1991) Heat-capacity measurements and thermodynamic functions of crystalline α-D-glucose at temperatures from 10 K to 340 K. J Chem Thermodyn 23:403–409. doi:10.1016/s0021-9614(05)80128-4
33. Putnam RL, Boerio-Goates J (1993) Heat-capacity measurements and thermodynamic functions of crystalline sucrose at temperatures from 5 K to 342 K—revised values for $\Delta_f G_m$ (sucrose, cr, 298.15 K), $\Delta_f G_m$ (sucrose, aq, 298.15 K), S_m (sucrose, cr, 298.15 K); and $\Delta_r G_m$ (298.15 K) for the hydrolysis of aqueous sucrose. J Chem Thermodyn 25:607–613. doi:10.1006/jcht1993.1055
34. da Silva MAVR, da Silva MDMCR, Ferreira AIMCL, Shi Q, Woodfield BF, Goldberg RN (2013) Thermochemistry of α-D-xylose(cr). J Chem Thermodyn 58:20–28. doi:10.1016/j.jct.2012.09.028
35. Voitkevich OV, Kabo GJ, Blokhin AV, Paulechka YU, Shishonok MV (2012) Thermodynamic properties of plant biomass components. Heat capacity, combustion energy, and gasification equilibria of lignin. J Chem Eng Data 57:1903–1909. doi:10.1021/je2012814
36. Goring DAI (1963) Thermal softening of lignin, hemicellulose and cellulose. Pulp Pap Mag Can 64:T517–T527
37. Orford PD, Parker R, Ring SG (1990) Aspects of the glass-transition behavior of mixtures of carbohydrate of low molecular-weight. Carbohydr Res 196:11–18. doi:10.1016/0008-6215(90)84102-z
38. Noel TR, Parker R, Ring SG (2000) Effect of molecular structure and water content on the dielectric relaxation behaviour of amorphous low molecular weight carbohydrates above and below their glass transition. Carbohydr Res 329:839–845. doi:10.1016/s0008-6215(00)00227-5
39. Liu YT, Bhandari B, Zhou WB (2006) Glass transition and enthalpy relaxation of amorphous food saccharides: a review. J Agric Food Chem 54:5701–5717. doi:10.1021/jf060188r
40. Paes SS, Sun SM, MacNaughtan W, Ibbett R, Ganster J, Foster TJ, Mitchell JR (2010) The glass transition and crystallization of ball milled cellulose. Cellulose 17:693–709. doi:10.1007/s10570-010-9425-7
41. Chen W, Lickfield GC, Yang CQ (2004) Molecular modeling of cellulose in amorphous state. Part I: model building and plastic deformation study. Polymer 45:1063–1071

42. Gierlinger N, Schwanninger M (2007) The potential of Raman microscopy and Raman imaging in plant research. Spectrosc Int J 21:69–89
43. Gierlinger N, Burgert I (2006) Secondary cell wall polymers studied by confocal Raman microscopy: spatial distribution, orientation, and molecular deformation. New Zeal J For Sci 36:60–71
44. Blackwell J, Vasko PD, Koenig JL (1970) Infrared and Raman spectra of cellulose from cell wall of *Valonia ventricosa*. J Appl Phys 41:4375–4379
45. Pandey KK, Pitman AJ (2003) FTIR studies of the changes in wood chemistry following decay by brown-rot and white-rot fungi. Int Biodeter Biodegr 52:151–160
46. Colom X, Carrillo F, Nogues F, Garriga P (2003) Structural analysis of photodegraded wood by means of FTIR spectroscopy. Polym Degrad Stab 80:543–549. doi:10.1016/s0141-3910(03)00051-x
47. Salmen L, Åkerholm M, Hinterstoisser B (2005) Two-dimensional Fourier transform infrared spectroscopy applied to cellulose and paper. In: Dumitriu S (ed) Polysaccharides: structural diversity and functional versatility. Marcel Dekker, New York, pp 159–187
48. Hofstetter K, Hinterstoisser B, Salmen L (2006) Moisture uptake in native cellulose—the roles of different hydrogen bonds: a dynamic FT-IR study using Deuterium exchange. Cellulose 13:131–145
49. Edwards HGM, Farwell DW, Williams AC (1994) FT-Raman spectrum of cotton—a polymeric biomolecular analysis. Spectrochim Acta A 50:807–811. doi:10.1016/0584-8539(94)80016-2